Debris Disk Structures Induced by Terrestrial-Mass Planets

Christopher Stark
University of Maryland
starkc@umd.edu

Marc Kuchner
NASA Goddard Space Flight Center
Marc.Kuchner@nasa.gov

Three-body models of dust dynamics suggest that extrasolar planets can create significant resonant structures in exozodiacal clouds and other debris disks. These structures are a worrisome source of confusion for missions that aim to directly detect extrasolar planets. So far, most models of these resonant structures have focused on Neptune- and Jupiter-mass planets[1-4]. **However, our simulations suggest that, under the right conditions, terrestrial-mass planets can also create high-contrast structures.** Using a custom tailored hybrid symplectic integrator on the 420-node Thunderhead cluster at Goddard Space Flight Center, we have performed many simulations of 25,000 particles each in an effort to catalog these structures. The models incorporate a realistic size distribution of particles and include enough particles to overcome the limitations of previous simulations that were often dominated by a handful of long-lived particles. These high-fidelity simulations allow us to confidently predict the contrast in the resulting ring structures.

Signatures of Terrestrial Planets

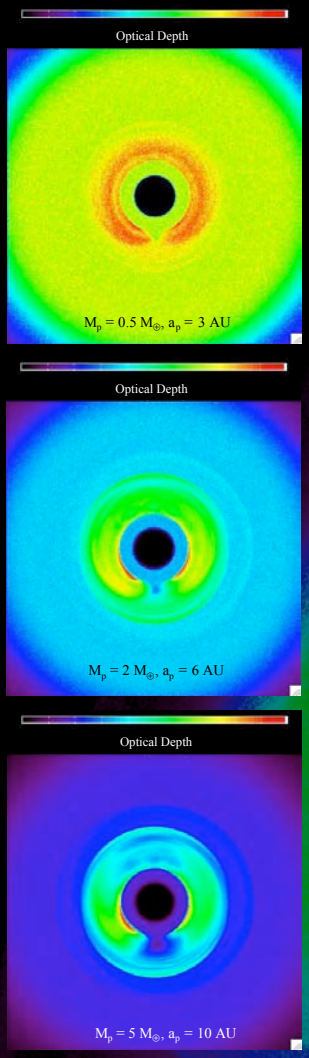

Our zodiacal cloud consists of small (~10-100 μm) dust grains, likely created by collisions between asteroids or Kuiper belt objects, and by comets. The smallest grains are ejected from the system while larger particles remain in orbit and slowly spiral inwards toward the host star due to Poynting-Robertson (PR) drag. As the particles spiral inwards, they can become trapped in mean motion resonances (MMRs) with planets, significantly extending their lifetimes. This prolonged trapping can produce a density structure in the dust disk.

Extrasolar debris disks with low enough optical depth should show patterns created by these kinds of resonant interactions, too.

We have performed over 100 simulations to date spanning 5 planetary mass values (0.1 - 5.0 $M_\oplus$), 4 planet semimajor axis values (1 - 10 AU), and 5 values of β (0.0023 - 0.23), equivalent to silicate particles 1.2 - 120 μm in radius. Each simulation considered 5,000 particles.

We created the images shown here by combining the results of all values of β, resulting in 20 simulations of 25,000 particles. We assumed a Dohnanyi distribution of particle sizes ($dN/dr \propto r^{-3.5}$) and took into account the scattering cross section.

As defined by Kuchner et al[5], this is a Type I structure due to the low mass and low eccentricity of the planet.

The particles were released on dynamically "cold" orbits with inclinations distributed between 0 and 20°, eccentricities between 0 and 0.2, and semimajor axes ranging from $3.5a_p$ to $4.5a_p$. We have not yet considered dust on dynamically "hot" orbits.

Our highest contrast case simulated is a 5 Earth-mass planet orbiting the Sun at 10 AU--this gives a contrast at the inner edge of the ring of nearly 8:1!

In all of the images shown, the planets are orbiting counter-clockwise. PR drag causes the asymmetry in ring structure--the pericenters of the dust in the direction trailing the planet are closer than those leading the planet.

Contrast vs. Planet Mass

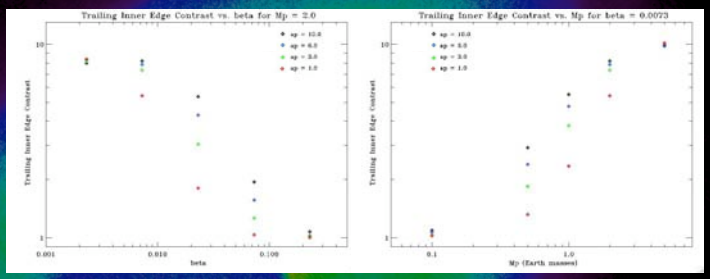

The ring structure is predominantly composed of dust particles in the 2:1 and 3:2 resonances. These resonances both have a pericenter of $\approx 0.83a_p$ creating a well-defined inner edge for the ring. Typically the highest contrast of the ring can be found at the inner edge trailing the planet. We azimuthally averaged a 90° swath trailing the planet and plotted the inner edge contrast vs. planet mass and beta, shown above. Both graphs show a transition between the no-trapping case and saturation. The contrast of the ring tells us about the nature of trapping probability. Note that several other measurements of contrast (leading inner edge, maximum contrast, radially averaged, etc.) give similar results.

Tests of our Integrator

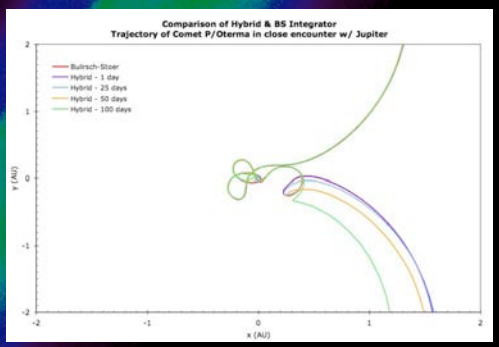

Our simulations were performed using a custom-tailored hybrid symplectic integrator. Our integrator, based on the techniques used by John Chambers in his MERCURY code[6], handles close encounters by effectively switching to a Bulirsch-Stoer integrator for the relevant bodies. We tested our integrator and showed that it exhibits no long term build-up in energy error (or Jacobi constant for the three body problem), correctly implements PR drag, and accurately handles close encounters. The trajectory of a comet in a close-encounter with Jupiter is shown above. We directly compare our integrator to a Bulirsch-Stoer integtrator. The results closely mirror those obtained by Chambers.

A direct comparison of density histograms for a Bulirsch-Stoer integrator (left) and our hybrid symplectic integrator (middle). The simulation consisted of 1,000 particles in the Sun-Earth system. Differences between the two images are within the limits of Poisson noise (right).

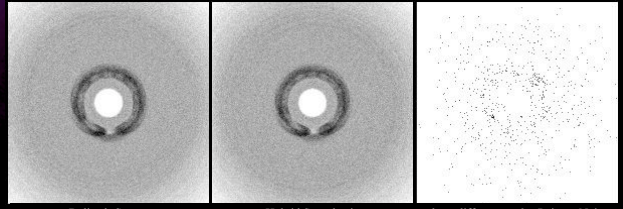

Bulirsch-Stoer | Hybrid Symplectic | where difference > 2 x Poisson Noise

References

1. Liou, J.-C. & Zook, H.A. Signatures of the giant planets imprinted on the Edgeworth-Kuiper belt dust disk. *AJ* **118**, 580-590 (1999).
2. Moro-Martin, A. & Malhotra, R. Dynamical models of Kuiper belt dust in the inner and outer solar system. *AJ* **125**, 2255-2265 (2003).
3. Moro-Martin, A. & Malhotra, R. A study of the dynamics of dust from the Kuiper belt: spatial distribution and spectral energy distribution. *AJ* **124**, 2305-2321 (2002).
4. Deller, A.T. & Maddison, S.T. Numerical modelling of dusty debris disks. *ApJ* **625**, 398-413 (2005).
5. Kuchner, M.J. & Holman, M.J. The geometry of resonant signatures in debris disks with planets. *ApJ* **588**, 1110-1120 (2003).
6. Chambers, J.E. A hybrid symplectic integrator that permits close encounters between bodies. *MNRAS* **304**, 793-799 (1999).